EXPERIMENTAL STUDY ON STRUCTURAL PERFORMANCE OF RC SHEAR WALL WITH L SHAPED SECTION

Go Hosaka[1], Hidetaka Funaki[2],
Hiroshi Hosoya[2] and Hiroshi Imai[3]

[1] *Graduate student, Dept. of Engineering Mechanics and Energy, University of Tsukuba, Ibaraki, Japan*
[2] *Technical Research Institute, Okumura Corporation, Japan*
[3] *Professor, Dept. of Engineering Mechanics and Energy, University of Tsukuba, Ibaraki, Japan*
Email: hosaka@rcs.kz.tsukuba.ac.jp

ABSTRACT :

Recently, many high-rise buildings with the center core structure system having high strength reinforced concrete shear walls have been constructed in Japan. Severe earthquake design forces cause huge bending moment and axial load at the bottom of the walls. Especially in the shear walls with L shape section, the improvement of compression ductility at the corner of the wall is needed. This paper aims to observe the structural performance of the L shape walls and to investigate the correspondence between experimental and analytical results by section analysis using fiber model. In this study, four specimens of 1/6-scale were produced, and horizontal shear loads were applied under varied axial loads. Parameters are concrete strength and bar arrangement. The corner part was confined by the lateral reinforcing bars. The analytical and the experimental results showed a good correspondence.

KEYWORDS: Shear wall with L shape section, Varied axial load, Section analysis by fiber model.

1. INTRODUCTION

Recently, as the demand of apartment housings increase, many super high-rise reinforced concrete structures have been constructed in Japan. To satisfy the requirements of higher degree of free floor plan of the buildings, the center core structure system with reinforced concrete shear walls is widely used. Severe earthquake design forces cause huge bending moment and axial load at the bottom of the walls. Especially in the shear walls with L shape section, the improvement of compression ductility at the corner part of the wall is needed. The objectives of this study are to observe the structural performance of the L shape walls and to investigate the correspondence between the experimental and the analytical results by section analysis using fiber model.

2. OUTLINE OF SPECIMENS

2.1 Specimens

Four specimens of 1/6-scale, which corresponded to the bottom portion of reinforced concrete model building of 30 stories, were produced. They were named as L-1, L-2, L-5 and L-6. The list of specimens is shown in Table 1, and the arrangement of the reinforcing bars is shown in Fig. 1. The wall is 134 mm deep, 670 mm long and 1940 mm high, and the loading height is 2140 mm. All specimens were designed as flexural failure mode.

Parameters of the experiment are concrete strength and bar arrangement. The concrete strength of L-5 is 80 N/mm^2, the others are 60 N/mm^2. At the corner and edge parts, the concrete are confined by high dense lateral reinforcements as column hoops. Confinement areas at the corner parts are 2D (D: Depth of the wall). Those at the edge parts of L-1 and L-2 are 2D, and those of L-5 and L-6 are 1D. In addition, although the confinement areas at the corner part of L-5 and L-6 are 2*D*, those are divided into every 1*D* and confined separately. The main reinforcing bars D10 (SD390) are arranged at the confinement areas. In addition, at the confinement areas of L-5 and L-6, the axial core bars are arranged to cover the reduced parts of confinement areas. The vertical and horizontal wall bars D6 (SD390) are arranged at the unconfined area between corner and edge parts. The lateral reinforcing bars of L-5 and L-6 are high strength bars D4 (USD785), the others are normal strength bars D4 (SD295).

Table 1 List of specimens

Specimen name	L-1	L-2	L-5	L-6
Depth of the wall, *D* (mm)	134			
Length of the wall, *L* (mm)	670			
Height of the wall, *h* (mm)	1940			
Loading height, *H* (mm)	2140			
Specified concrete strength, F_c (N/mm^2)	60	60	80	60
Axial stress ratio for long term	0.15			
Axial stress ratio for short term	0 - 0.40	0 - 0.40	0 - 0.40	0 - 0.45
Spacing of the lateral reinforcing bar at the corner part (mm)	40	30	40	40

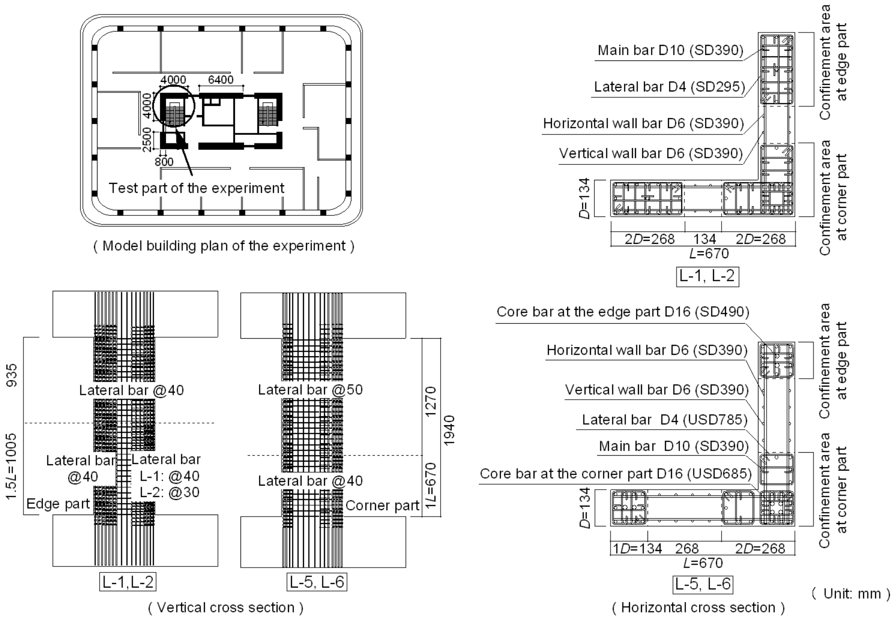

Figure 1 Arrangement of the reinforcing bars

2.2 Material test

The material test results of concrete and reinforcing bars are shown in Tables 2 and 3, respectively. Each value is the average of three specimens.

Table 2 Material test result of concrete

Specimen	Elastic coefficient E_c (GPa)	Compressive strength σ_B (MPa)	Splitting strength σ_t (MPa)	Material age at experiment
L-1	31.5	58.9	4.24	50 days
L-2	37.0	67.1	4.62	39 days
L-5	37.8	89.8	4.16	69 days
L-6	32.7	65.5	4.12	62 days

Table 3 Material test result of reinforcing bars

Specimen	Type	Elastic coefficient E_s (GPa)	Yield strength σ_y (MPa)	Yield strain ε_y (%)	Tensile strength σ_t (MPa)
L-1	D4 (SD295)	180	388	0.22	531
	D6 (SD390)	172	421	0.25	568
	D10 (SD390)	172	431	0.28	588
L-2	D4 (SD295)	193	401	0.20	559
	D6 (SD390)	191	486	0.25	631
	D10 (SD390)	191	410	0.22	638
L-5 L-6	D4 (USD785)	183	927	0.51	1027
	D6 (SD390)	188	446	0.24	617
	D10 (SD390)	186	435	0.23	600
	D16 (SD490)	189	538	0.29	698
	D16 (USD685)	193	733	0.38	921

*Note D10: Deformed bar with 10 mm of diameter
SD390: Specified yield strength of 390 N/mm^2

3. METHOD OF LOADING

Loading system is shown in Fig. 2. Axial load was applied by vertical actuators, and static cyclic shear load was applied by horizontal actuator. Shear load was controlled by deformation angle R, which was the horizontal relative displacements between upper and lower stubs divided by loading height H. Axial load was simplified as shown in Fig. 2 and controlled in correspondence to the shear load. Axial load of L-6 was varied from 0 to 0.45 in terms of compressive stress ratio, those of the others were varied from 0 to 0.40. The horizontal loading direction was diagonal one. When the corner parts of the walls were compressed, axial stress ratio were set to the maximum.

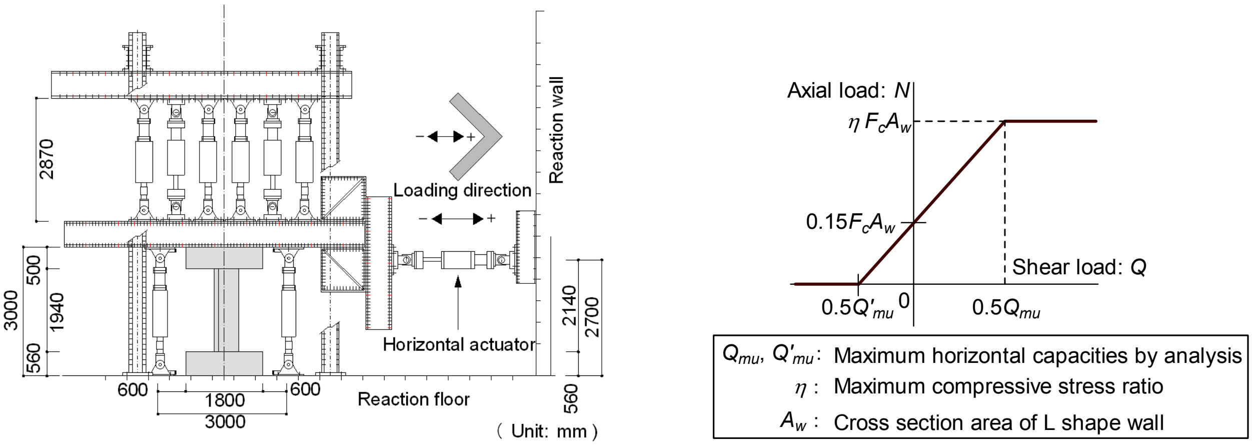

(Loading system) (Relationship between applied axial and shear loads)

Figure 2 Loading method

In this loading method, as the deformation angle *R* becomes large, actuators incline as shown in Fig. 3. The load in horizontal component arises when vertical actuators incline, so that additional bending moment arises at the bottom of specimen. In addition, it results in difference between the original loading height and the acting line of the horizontal actuator when it inclines, so that additional bending moment arises. It is defined that the sum of their additional bending moments divided by the original loading height *H* as additional shear load. Then, the shear load *Q* is compensated by adding the additional shear load to the measured load *Q'* of horizontal actuator.

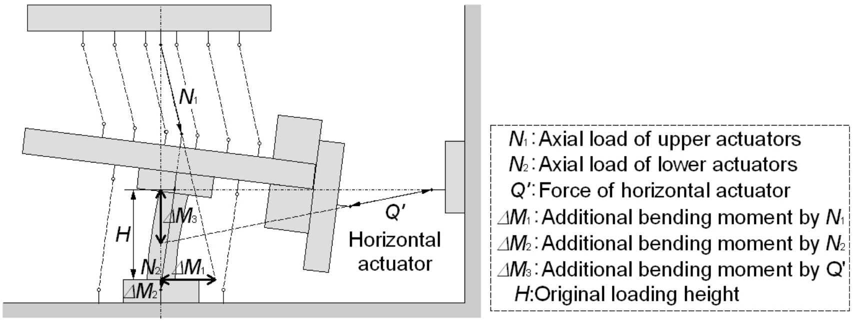

Figure 3 Conceptual diagram in compensating horizontal shear load

4. EXPERIMENTAL RESULT

4.1 Failure process and load-deformation angle relationships

Load-deformation angle (*Q*-*R*) relationships are shown in Fig. 4 and final crack patterns are shown in Fig. 5.

For L-1 and L-2 with F_c 60 of concrete strength, bending cracks occurred at the corner part of walls at *R*=-1/400. Compression failures happened at the corner part of the bottom of the walls at *R*=+1/200, and main reinforcing bars at the corner part yielded in compression. The compression failures developed to the middle of the walls at *R*=+1/67. The maximum shear loads were observed at *R*=+1/33, and then those decreased.

For L-5 (F_c 80), bending cracks occurred at the corner part of walls at *R*=-1/800. Compression failure happened at the bottom corner part of the wall at *R*=+1/200. Main bars at the corner part yielded in compression at *R*=+1/200, and those at the edge part yielded in tension at *R*=+1/67. The maximum shear loads were observed in ± *R*=1/33 in both positive and negative loadings.

The failure process of L-6 (F_c 60) showed the same as L-5, the maximum shear loads were also about same. As compared with L-1 and L-2, it showed the almost same in the positive loading, but about 1.5 times value in the negative loading.

In addition, for L-5, in spite of using higher concrete strength than others, the maximum shear load showed the about same. One of the reasons is considered that by dividing confinement area at the corner part (2*D*) into every 1*D*, the lateral bars lacked at the confinement areas, then vertical shear cracks at the bottom corner part of the wall occurred by the large axial load as shown in Fig. 5, and the horizontal load didn't increase. Another is considered that the concrete might not be fully compacted at the corner and the edge of the wall in the specimen, because the reinforcing bar arrangement was overcrowded at the confinement areas by arranging the axial core bars.

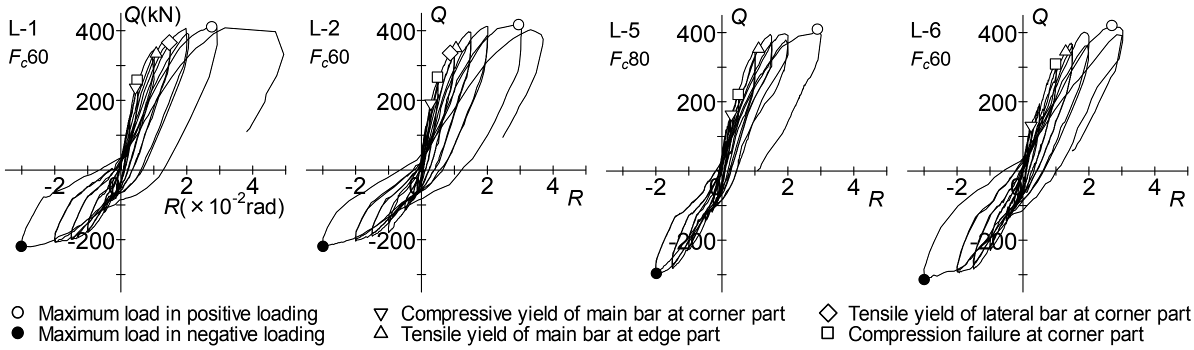

Figure 4 Load-deformation angle (Q-R) relationships

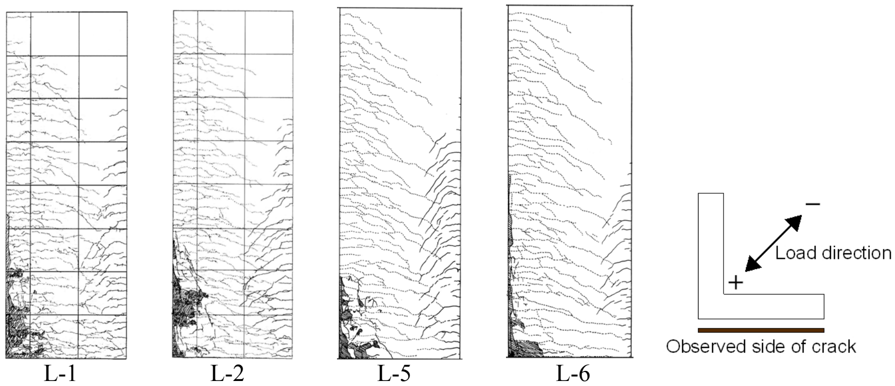

Figure 5 Final crack patterns

4.2 Strain distribution in main reinforcing bars

Strain distributions in the main reinforcing bars at the section 20 mm high from bottom of the walls in the positive loading are shown in Fig. 6.

All specimens show the almost same strain distribution patterns. The strain distributions are almost linear with the small deformation angles, so that the assumption is well made up that linear section before deformation remains linear after deformation. At R=+1/200, the main bars at the corner part yielded in compression, then the strains increased. In addition, for L-5 and L-6, although the axial core bars were arranged at corner and edge parts of the walls, the strain distributions showed the same as L-1 and L-2. The axial core bars showed high stress by considering strain developments of the main bars around them, so that it is considered that the axial core bars contribute to the increase of flexural bearing capacity.

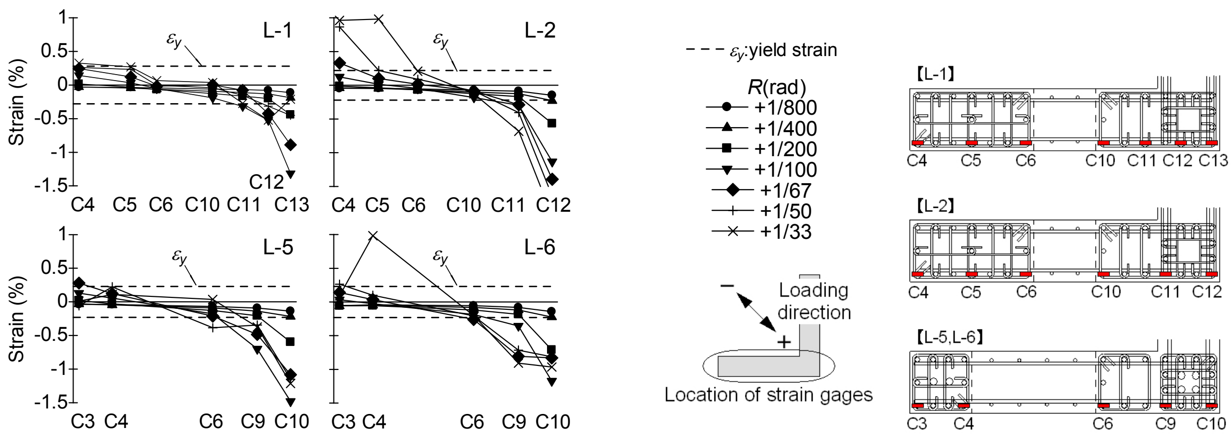

Figure 6 Strain distributions of main reinforcing bars

4.3 Strain distribution in lateral reinforcing bars

Strain distributions in lateral reinforcing bars at the section 40 mm high from bottom of the walls in the positive loading are shown in Fig. 7.

For all specimens, the strains of lateral reinforcements at the corner part that were compressed in the positive loading increased. On the other hand, those at the edge part that were compressed in the negative loading didn't increase so much. For L-1 and L-2, the normal strength lateral reinforcements (SD295) reached the yield strains in the last cycle of loading. On the other hand, for L-5 and L-6, the high strength lateral reinforcements (USD785) showed high stress and confined the corner parts sufficiently, but they remained in the elastic range. It is considered that the confinement effects that corresponds to their yield strength couldn't be obtained.

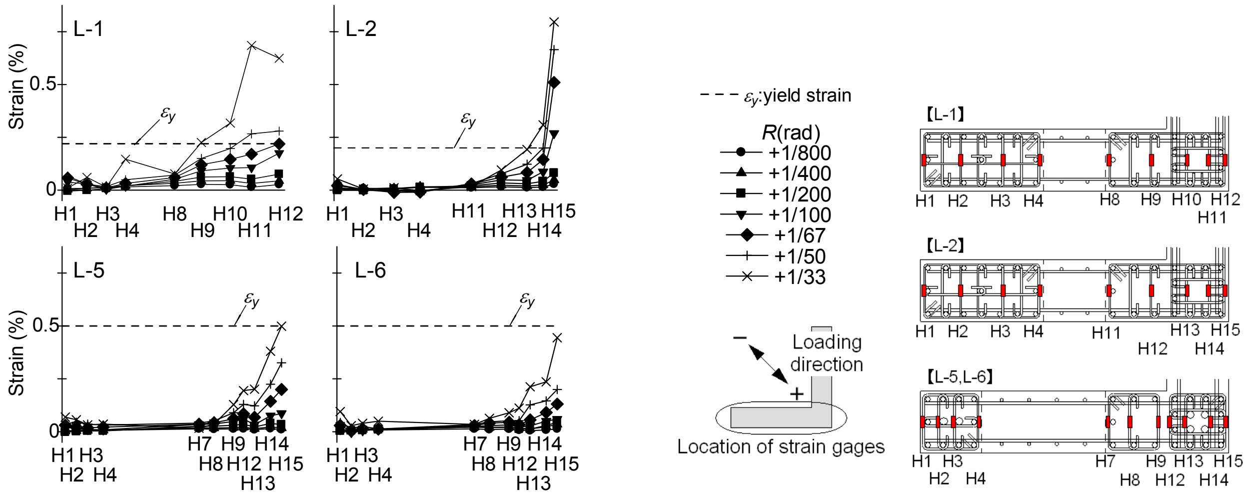

Figure 7 Strain distributions of lateral reinforcing bars

4.4 Flexural and shear deformations

Specimen is divided into 5 parts (I_0-I_4) as shown in Fig. 8. The flexural and shear deformations in each part were measured by displacement sensors arranged as a truss. The horizontal displacement at the loading height is defined as total deformation, and the ratios of deformations at the each part are shown in Fig. 9. Bold lines show the border between flexural and shear deformations.

For all specimens, flexural deformations occupied more than 90% of total deformations. Those at the sections about 1*L* from the bottom of the walls (I_0-I_2) were especially dominant, and occupied 80% of total deformations in the final stage.

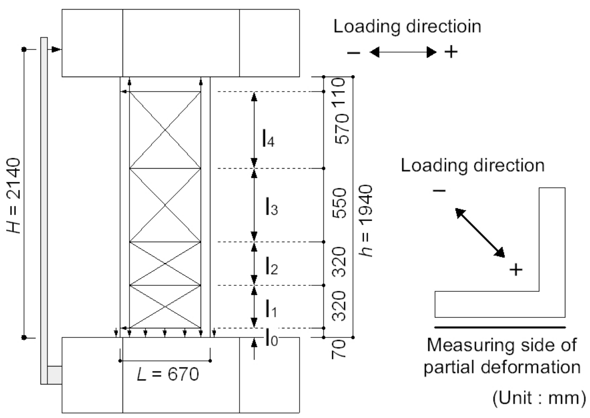

Figure 8 Measurement segments of partial deformations

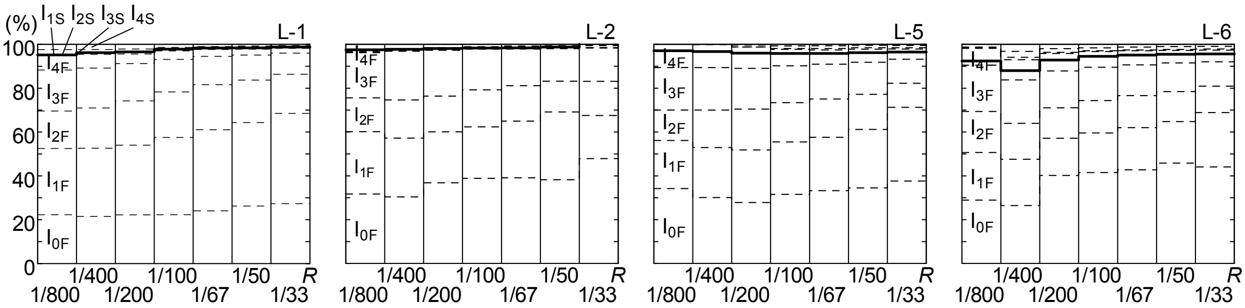

*Subscript F and S indicate flexural and shear deformations, respectively.

Figure 9 Ratios of flexural and shear deformations at segments

5. SECTION ANALYSIS

Section analysis is performed by fiber model with supposing that the strain distribution is linear. For reinforcing bar, perfect elastic-plastic type model is used for the stress-strain relationship. For concrete, Kent-Park model [1], that is modified, is used. Original Kent-Park model doesn't correspond to high strength concrete as used in this experiment, so the modified model shown in Fig. 10 is used. In original Kent-Park model, the strain ε_0 at the maximum stress is defined 0.2% at both confined and unconfined areas. In the modified model, Eqns. 5.1 and 5.2 [2] are used for ε_0 at the confined area, so that the increase of strain by lateral confinement is appropriately evaluated. In addition, the strain of cylindrical test piece at the maximum compressive strength is used for ε_0 at the unconfined area.

$$\varepsilon_{c0} = \varepsilon_0 \begin{cases} 1 + 4.7(K-1) & (K \leq 1.5) \\ 3.35 + 20(K-1.5) & (K > 1.5) \end{cases} \tag{5.1}$$

$$K = \sigma_{cB} / \sigma_B \tag{5.2}$$

σ_{cB} : Tri-axial compressive strength of concrete σ_B : Concrete strength of cylindrical test piece

In addition, σ_{cB} is obtained by Eqns. 5.3 and 5.4.

$$\sigma_{cB} = \sigma_p + k\sigma_l \tag{5.3}$$

$$\sigma_l = 0.5\sigma_{wy} p_w \tag{5.4}$$

σ_p: Uni-axial compressive strength of concrete(=σ_B) k : Constant (6 for high strength concrete)
σ_{wy} : Yield strength of lateral reinforcement p_w : Ratio of lateral reinforcement

Although yield strength σ_{wy} of lateral reinforcement was used in Eqn. 5.4, for L-5 and L-6, the lateral reinforcing bars didn't yield. Therefore, average stress of the lateral reinforcements in the last cycle of loading ($\cong 0.40\ \sigma_{wy}$) was used in place of yield strength. In addition, although uni-axial compressive strength σ_p of concrete is often defined as $\sigma_p = 0.85\sigma_B$ by reduction coefficient 0.85 in the application to actual size, it is defined $\sigma_p = \sigma_B$ by considering reduced specimens in this study.

Moment-curvature (M-ϕ) relationships at the bottom of the walls, that is compared with the analytical results, are shown in Fig. 11. For all specimens, shapes of analytical M-ϕ curves simulate the experimental results well by using modified model. For L-1, although a little difference between the experimental and the analytical curves is observed in the last cycle of positive loading, initial stiffness and whole shape of M-ϕ curve show a good correspondence well until R=+1/33. The analytical result is well correspondent to the experimental one, although the analytical result slightly falls below the experimental. For L-2, the analytical result also evaluates the experimental result well. For L-5, the analytical result exceed the experimental. The reason is considered the development of the vertical shear cracks and the problem of concrete not enough to be compacted by the overcrowded bar arrangement as noted above. For L-6, the analytical result evaluates the experimental one well by considering appropriately the confinement effect of the lateral reinforcements. In addition, for all specimens, the analytical results can evaluate the experimental ones well in the negative loading, although the analytical slightly fall below the experimental.

Until maximum stress

$$\sigma_c = \sigma_{cB}\left\{2(\varepsilon_c/\varepsilon_{c0}) - (\varepsilon_c/\varepsilon_{c0})^2\right\}$$

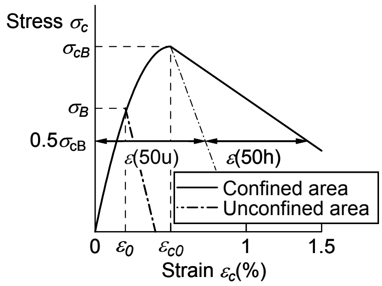

After maximum stress

$$\sigma_c = \sigma_{cB}\left(1 - \frac{0.5(\varepsilon_c - \varepsilon_{c0})}{\varepsilon(50h) + \varepsilon(50u) - \varepsilon_{c0}}\right)$$

$$\begin{cases} \varepsilon(50u) = \dfrac{0.21 + 0.002\sigma_B}{\sigma_B - 70} + (\varepsilon_{c0} - 0.002) \quad (\sigma_B : kgf/cm^2) \\ \varepsilon(50h) = 0.75\rho_h\sqrt{b_c/s} \end{cases}$$

P_h: Volume ratio of lateral reinforcement
b_c: Short side length of lateral reinforcement
s: Spacing of lateral reinforcement

Figure 12 Modified model

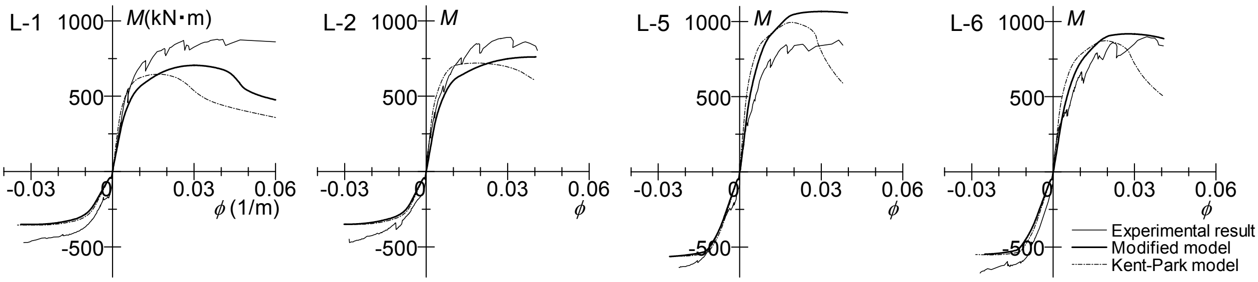

Figure 13 Moment-curvature relationships

6. CONCLUSION

The structural performance of reinforced concrete shear walls with L shape section was investigated. The section analysis was performed by using fiber model. The followings are summarized.

(1) Flexural deformations at the sections about 1L from the bottom of the walls (I_0-I_2) were especially dominant, and those finally occupied 80% of total deformations.
(2) The strain developments of the main reinforcing bars had no difference whether the core reinforcing bars at the confinement areas were arranged or not.
(3) The high strength lateral reinforcing bars didn't yield, so the confinement effects that correspond to their yield strength couldn't be obtained.
(4) The analytical results using fiber model with supposing the linear strain distribution can evaluate the experimental results well.

REFERENCES

[1] Scott, B. D., Park, R., and Priestley, M. J. N. (1982). Stress-strain behavior of concrete confined by overlapping hoops at low and high strain rates. *ACI J.*, **No.1**, pp13-27.
[2] Sakino, K. and Sun, Y. (1994). Stress-strain curve of concrete confined by rectilinear hoop. *J. Struct. Constr. Eng. AIJ,* **No.461,** pp95-104.